Electronic Supplementary Information

Coordination Cages as Tunable Ligands for the Synthesis of Porous Salts

Qiong Zhou,[a] Nobuyuki Yamamoto,[a] Dewni D. Fernando,[a] Yaroslav Losovyj[a,b], Alex Lovstedt,[a] and Eric D. Bloch*[a]

[a]Department of Chemistry, Indiana University, Bloomington, Indiana 47405, United States

[b]Department of Physics and Astronomy, University of Nebraska, Lincoln, Nebraska 68588, United States

Table of Contents

Detailed Experimental 3
Materials and Methods 3
Synthesis of Zr-based cages 3
Porous salt formation 4
Gas adsorption measurements 5
Supporting Tables 6
Supporting Figures 8
References 26

Experimental

A. General considerations

Materials All reagents were obtained from commercial vendors. Anhydrous solvents were dispensed from a Pure Process Technology solvent system and stored in a nitrogen glovebox over 4 Å molecular sieves. NMR solvents were purchased from Sigma-Aldrich.

Characterization Single crystal X-ray diffraction measurements were collected on a Bruker Venture D8 diffractometer equipped with a Photon III detector at 173(2) K. Powder X-ray diffraction (PXRD) patterns were measured on an Empyrean diffractometer with Cu Kα radiation (λ = 1.5419 Å, 45 kV, 40 mA). The 2θ scan range was from 4° to 60° with a step size of 0.0167° and a measurement time of 200 s per step. Simulated PXRD patterns were calculated from the corresponding single crystal structures using Mercury software.
Proton (^{1}H) NMR spectra were recorded on the Varian I400 (400 MHz), I500 (500 MHz) spectrometers, and the Bruker 500 MHz Avance Neo NMR spectrometer. ^{13}C NMR spectra were recorded on the Bruker 500 MHz Avance Neo NMR Spectrometer. The spectra were referenced against the solvent residual peak: deuterated dimethyl sulfoxide (DMSO-d_6) (2.50 ppm, ^{1}H), deuterated methanol (MeOH-d_4) (3.31 ppm, ^{1}H). The digested NMR was carried out by adding CsF (dissolved in D_2O) or DCl to the NMR samples.
Infrared spectra were collected on a Bruker Alpha II FT-IR in the range of 4000-400 cm^{-1}.
Thermal gravimetric analysis (TGA) was conducted on a TA Instruments TGA 5500. Samples were heated to 600 °C at 5 °C/min under a simulated air atmosphere of 20% O_2 and 80% N_2.
X-ray photoelectron spectroscopy (XPS) measurements were carried out on the PHI VersaProbe II Scanning X-ray Microprobe system.
Mass spectroscopy (MS) measurements were conducted on SYNAPT G2-S mass spectrometer. The cage samples were dissolved in MeOH and filtered through 0.2 µm filters, with the m/z range from 400 to 2000 Da.
UV-vis spectra were collected using a Jasco V750 UV-visible Spectrophotometer with continuous scan spectra obtained from 300 nm to 900 nm at a scan rate of 400 nm/min and step size of 0.5 nm for solutions. Diffuse reflectance UV-Vis spectra were collected with a 60 mm diameter integrating sphere for solids samples.

B. Cage synthesis

Na-bound cage The synthesis procedure was adapted from literature[1]. In a 20 mL scintillation vial, Cp_2ZrCl_2 (0.3 g, 1.026 mmol) and 5-SO_3Na H_2bdc (0.1 g, 0.373 mmol) were dissolved in 20 mL MeCN and 3 mL DI H_2O. The resulting solution was heated in a dry bath at 65 °C for 6 h before cooling slowly to room temperature. Clear crystals started to form after heating for about 2 h. The cage crystals were subjected to solvent exchange with 20 mL fresh MeCN over the course of 3 days, replacing the solvent once per day.

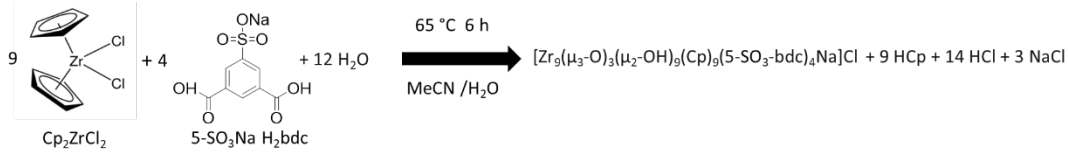

Li-bound cage In a 20 mL scintillation vial, Cp_2ZrCl_2 (0.3 g, 1.026 mmol) and 5-SO_3Li H_2bdc (0.1 g, 0.397 mmol) were dissolved in 20 mL MeCN and 3 mL DI H_2O. The resulting solution was heated in a dry bath at 65 °C for 6 h before cooling slowly to room temperature. Clear needle crystals started to form after heating for about 2 h. The cage crystals were subjected to solvent exchange with 20 mL fresh MeCN over the course of 3 days, replacing the solvent once per day.

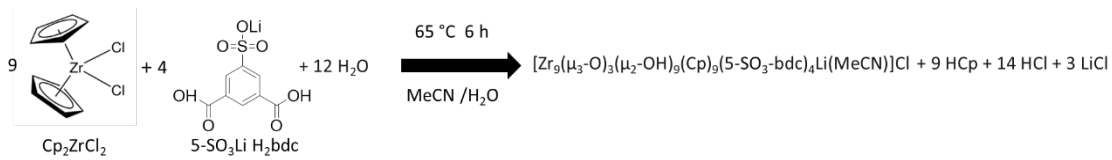

Free-pocket cage In a 20 mL scintillation vial, Cp_2ZrCl_2 (0.3 g, 1.026 mmol) and 5-SO_3Na H_2bdc (0.1 g, 0.373 mmol) were dissolved in 20 mL MeCN and 3 mL DI H_2O. 300 µL 15-crown-5 was added to the mixture. The resulting solution was heated in a dry bath

at 65 °C for 6 h before cooling slowly to room temperature. Clear crystals started to form after heating for about 2 h. The cage crystals were subjected to solvent exchange with 20 mL fresh MeCN over the course of 3 days, replacing the solvent once per day.

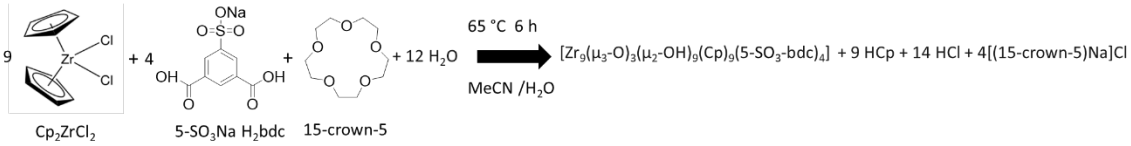

Tetrahedral Zr-dimethyl cage In a 20 mL scintillation vial, Cp_2ZrCl_2 (0.3 g, 1.026 mmol) and 2,5-dimethyl terephthalic acid (0.1 g, 0.513 mmol) were dissolved in 20 mL DMF and 0.5 mL DI H_2O. The resulting solution was heated in a dry bath at 65 °C for 18 h before cooling slowly to room temperature. The white cage solids were subjected to solvent exchange with fresh DMF over the course of 3 days, replacing the solvent once per day. The same washing procedure was repeated using $CHCl_3$.

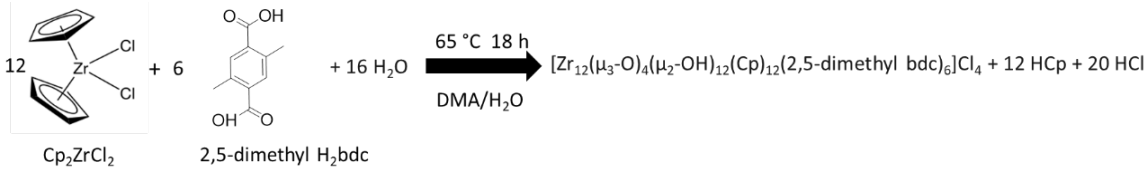

$Li_{24}[Mo_{24}(5\text{-}SO_3\text{-}bdc)_{24}]$ cage The synthesis procedure was published[2]. In a 20 mL scintillation vial, $Mo_2(OAc)_4$ (0.184 g, 0.432 mmol) and 5-SO_3Li H_2bdc (0.1088 g, 0.432 mmol) were dissolved in 12 mL of 9:1 DMA: MeOH solution. The resulting solution was heated in a dry bath at 95 °C for 2 days before cooling slowly to room temperature. 8 mL of diethyl ether was added to precipitate the bulk material. The precipitate was washed with MeCN and MeOH three times and dried under a dynamic vacuum to yield orange powder.

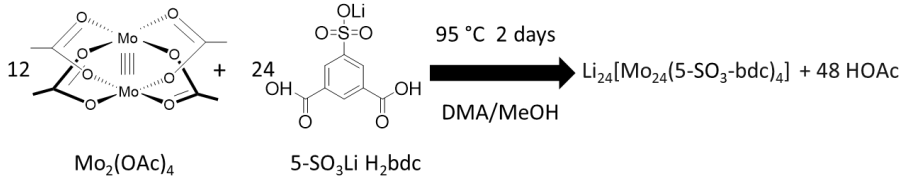

C. Porous salt formation

Fluorescent salt with Eosin Y In a 20 mL scintillation vial, Eosin Y disodium salt (10 mg) was mixed with free-pocket cage (100 mg) in 20 mL MeCN, and the mixture was stirred for 24 h. The resulting solids were washed with MeCN until the supernatant was colorless. The product was dried under a dynamic vacuum.

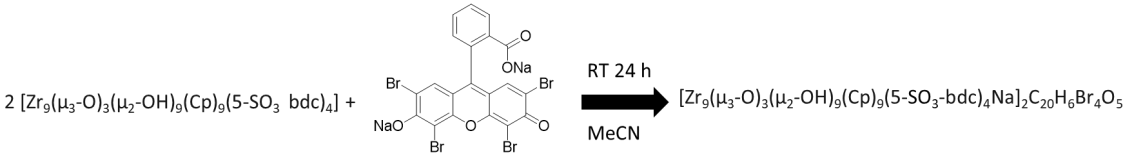

Salt with Li_2PdCl_4 In a 20 mL scintillation vial, Li_2PdCl_4(20 mg) was mixed with free-pocket cage (100 mg) in 20 mL MeOH, and the mixture was stirred for 24 h. The resulting solids were washed with MeOH until the supernatant was colorless. The product was dried under a dynamic vacuum.

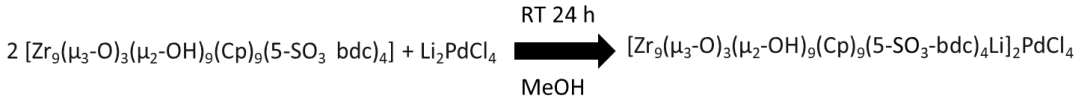

Salt with $Li_{24}[Mo_{24}(5\text{-}SO_3\text{-}bdc)_{24}]$ cage In a 20 mL scintillation vial, free-pocket cage (100 mg) was mixed with $Li_{24}[Mo_{24}(5\text{-}SO_3\text{-}bdc)_{24}]$ cage (30 mg) in 20 mL EtOH. The mixture was stirred for 24 h. The resulting solids were washed with EtOH and MeOH until the supernatant was colorless. The product was dried under a dynamic vacuum.

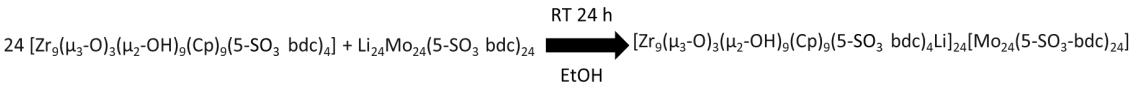

D. Gas adsorption and desorption

Gas adsorption isotherms were measured using Micromeritics Tristar II Plus and Micromeritics 3Flex. Samples were dried under dynamic vacuum and transferred into pre-weighed analysis tubes under 1 bar of helium (He). The samples were then vacuum-activated at the desired temperatures using a turbo vacuum system. After activation, the mass of the tubes with the activated samples was recorded. The analysis tubes were subsequently transferred to the analysis ports of the Tristar II Plus or 3Flex for gas adsorption measurements. Ultrahigh-grade gases were used for all isotherm experiments. Liquid nitrogen was used as the bath for N_2 isotherms at 77 K. Dry ice in isopropanol mixture was used as the bath for CO_2 isotherms at 195 K. Water bath with temperature control was used for isotherms at 298 K.

Cages	**Na-bound**	**Li-bound**	**Free-pocket**
Empirical formula	$C_{77}H_{68}ClNaO_{41}S_4Zr_9$, [+ solvent]	$C_{79}H_{69}ClLiNO_{40}S_4Zr_9$, [+ solvent]	$C_{79.50}H_{77.75}Cl_{0.50}N_{1.25}O_{44}S_4Zr_9$, [+ solvent]
Fw	2656.97	2663.96	2721.62
Crystal color, shape, size	colorless plate 0.171 × 0.089 × 0.021 mm³	colorless needle 0.503 × 0.129 × 0.067 mm³	colorless plate 0.409 × 0.235 × 0.084 mm³
Temperature	173(2) K	173(2) K	173(2) K
Wavelength	0.71073 Å	0.71073 Å	0.71073 Å
Crystal system, space group	Monoclinic, $P2_1/c$	Monoclinic, $P2_1/n$	Triclinic, P-1
a, Å	20.2784(13)	26.2825(16)	17.0323(15)
b, Å	16.8255(10)	29.9901(17)	26.088(2)
c, Å	36.624(2)	31.792(2)	34.411(3)
α, deg	90	90	77.641(2)
β, deg	100.3708(18)	95.7577(16)	79.161(2)
γ, deg	90	90	81.498(3)
V, Å³	12291.7(13)	24933(3)	14576(2)
Z	4	8	4
Dc, g/cm³	1.436	1.419	1.240
μ, mm^{-1}	0.892	0.876	0.744
Reflections collected	21327	632857	534155
θ range, deg	2.042 - 25.049	1.872 - 25.058	1.870 - 25.350
F (000)	5240	10512	5392
GOF on F^2	1.114	1.101	1.034
R1/wR2 (I > 2(I))	*R1 = 0.1218* *wR2 = 0.2917*	*R1 = 0.1039* *wR2 = 0.2229*	*R1 = 0.0513* *wR2 = 0.1309*
R1/wR2 (all data)	*R1 = 0.1961* *wR2 = 0.3139*	*R1 = 0.1356* *wR2 = 0.2513*	*R1 = 0.0649* *wR2 = 0.1454*
CCDC #	2475056	2475059	2475058

Table S1. Crystal structures and refinements of Na-bound, Li-bound and free-pocket cages.

element	band	Positions, eV	PosSep, eV	FWHM, G, eV	%Gauss	%Area	ChiSquared
Zr3d	1	182.3	0	1.58	100	59.9	2.2
	2	184.7	2.4	1.58	100	40.1	
S2p	1	168.0	0	1.98	84	66.7	1.1
	2	169.4	1.4	2.03	70	33.3	
Cl2p	1	198.6	0	2.7	80	66.7	1.5
	2	200.1	1.5	2.3	80	33.3	

Table S2. Zr3d, S2p and Cl2p XPS spectra fitting for Na-bound cage. All XPS binding energy was calibrated to C1s (284.8 eV).

element	band	Positions, eV	PosSep, eV	FWHM, G, eV	%Gauss	%Area	ChiSquared
Zr3d	1	182.5	0	1.6	100	59.9	1.7
	2	184.8	2.3	1.6	100	40.1	
S2p	1	168.1	0	2.1	70	66.7	1.8
	2	169.4	1.3	1.9	90	33.3	
Cl2p	1	198.6	0	2.2	100	66.7	1.1
	2	200.0	1.4	2.0	80	33.3	
element	band	Positions, eV	PosSep, eV	FWHM, G, eV	%Gauss	%Area	ChiSquared
Zr4s	1	53.5	/	2.9	70	90.7	1.1
Li1s	2	56.2	/	2.4	80	9.3	

Table S3. Zr3d, S2p and Cl2p XPS spectra fitting and Li1s deconvolution for Li-bound cage.

element	band	Positions, eV	PosSep, eV	FWHM, G, eV	%Gauss	%Area	ChiSquared
Zr3d	1	182.6	0	1.5	97	59.9	2.0
	2	184.9	2.3	1.5	98	40.1	
S2p	1	168.1	0	2.1	70	66.7	1.5
	2	169.4	1.3	1.8	90	33.3	

Cl2p	1	198.6	0	2.2	100	66.7	1.2
	2	200.0	1.4	2.4	80	33.3	

Table S4. Zr3d, S2p and Cl2p XPS spectra fitting for free-pocket cage.

Element ratios	S: Zr	Per cage (three Zr cluster)	Na (or Li): Zr	Per cage (three Zr cluster)	Cl: Zr	Per cage (three Zr cluster)
Na-bound cage	4.5:9	4	1.1:9	1	1.1:9	1
Li-bound cage	3.7:9	4	1.8:9	2	0.9:9	1
Free-pocket cage	4.3:9	4	0.1:9	0.1	1.2:9	1

Table S5. Element ratios calculated for Na-bound, Li-bound and free-pocket cages from XPS spectra.

element	band	Positions, eV	PosSep, eV	FWHM, G, eV	%Gauss	%Area	ChiSquared
Zr3d	1	181.3	0	2.03	88	51.5	2.0
	2	182.0	0.6	1.33	100	9.3	
	3	183.7	2.4	2.03	100	34.5	
	4	184.7	3.4	1.38	100	4.7	
Br3d	1	69.3	0	1.9	80	59.9	1.2
	2	70.8	1.5	2.2	80	40.1	

Table S6. Zr3d and Br3d XPS spectra fitting for salt made from free-pocket cage and Eosin Y.

element	band	Positions, eV	PosSep, eV	FWHM, G, eV	%Gauss	%Area	ChiSquared
Zr3p	1	332.2	0	3.5	97	44.7	1.8
	2	346.6	14.4	3.3	100	19.7	
Pd3d	3	336.3	0	3.2	80	13.2	
	4	341.5	5.2	3.2	100	22.4	

Table S7. Pd3d XPS spectra deconvolution for salt made from free-pocket cage and Li_2PdCl_4.

element	band	Positions, eV	PosSep, eV	FWHM, G, eV	%Gauss	%Area	ChiSquared
Zr3d	1	182.4	0	2.1	88	59.9	3.0
	2	184.8	2.4	2.1	80	40.1	
Mo3d	1	229.9	0	2.9	80	14.9	2.3
	2	233.3	3.4	2.0	90	10.0	
	3	232.1	0	2.1	80	45.0	
	4	235.3	3.2	2.3	60	30.2	

Table S8. Zr3d and Mo3d XPS spectra fitting for salt made from free-pocket cage and $Li_{24}[Mo_{24}(5\text{-}SO_3\text{-}bdc)_{24}]$ cage.

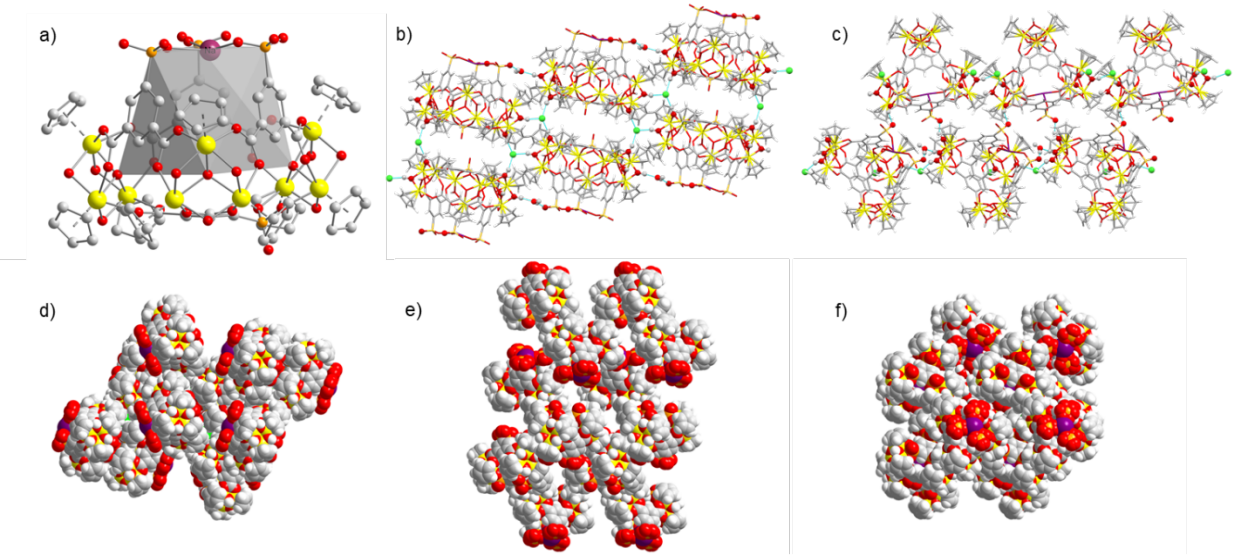

Figure S1. Crystal structure of Na-bound cage. (a) cage unit, (b) (c) key intermolecular interactions (H-bonds are cyan colored), and molecular packing viewed along d) *a*-axis, (e) *b*-axis, and (e) *c*-axis. Zr: yellow, O: red, C: grey, S: orange, Na: plum, Cl: green.

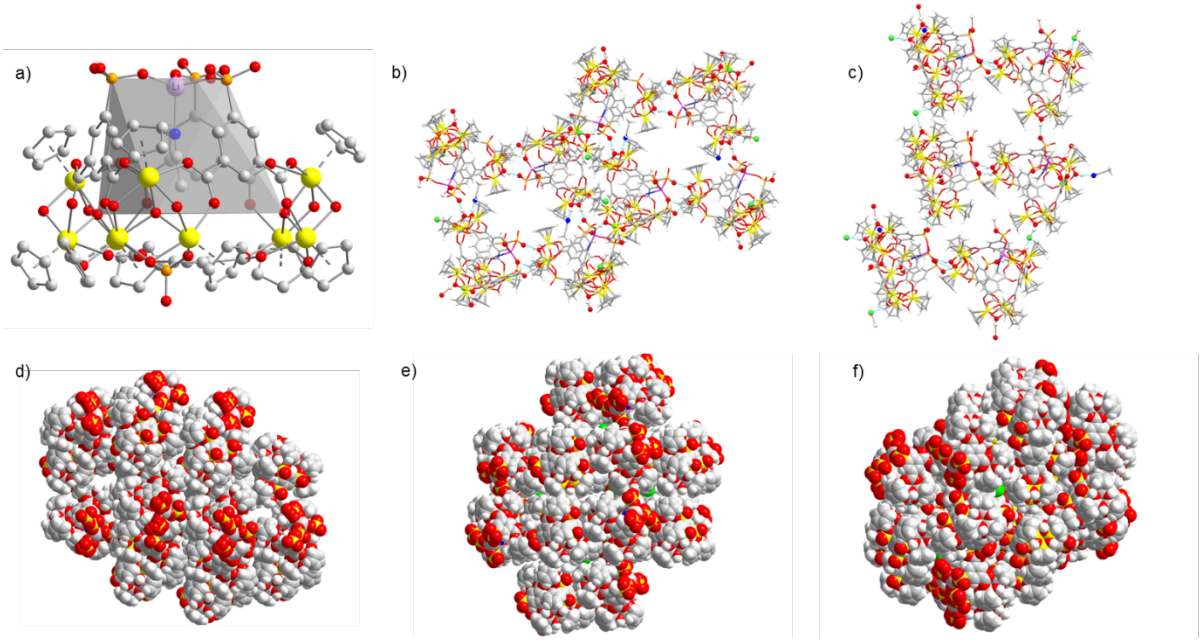

Figure S2. Crystal structure of Li-bound cage. (a) cage unit, (b) (c) key intermolecular interactions (H-bonds are cyan colored), and molecular packing viewed along d) *a*-axis, (e) *b*-axis, and (e) *c*-axis. Zr: yellow, O: red, C: grey, S: orange, Li: violet, N: blue, Cl: green.

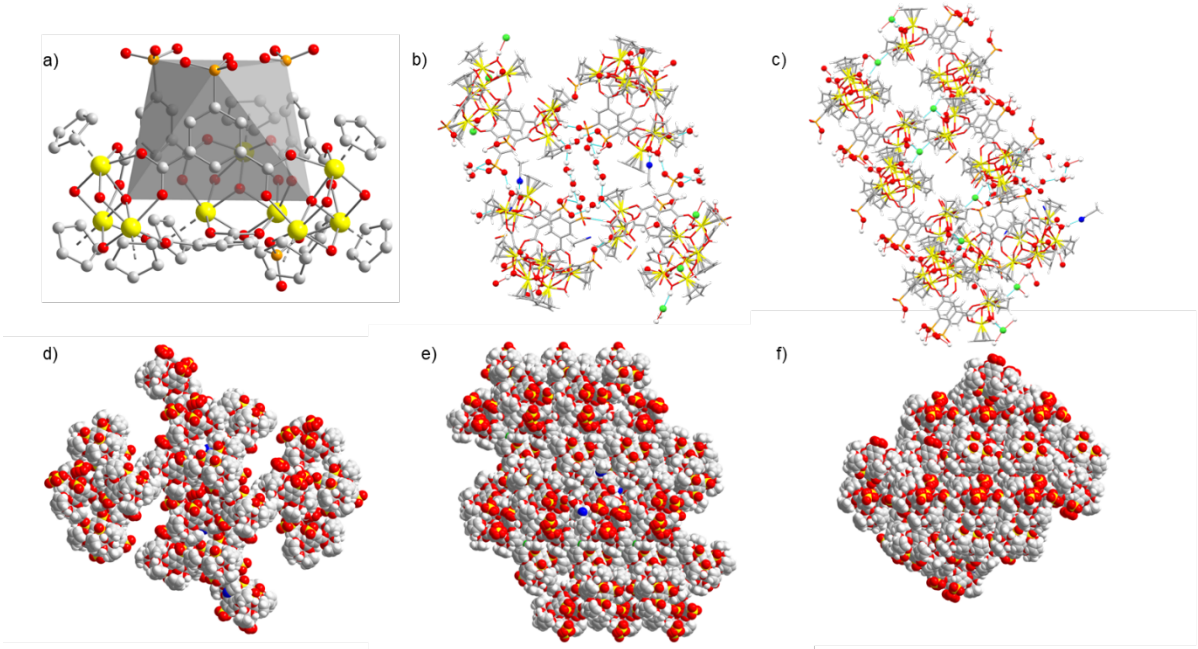

Figure S3. Crystal structure of free-pocket cage. (a) cage unit, (b) (c) key intermolecular interactions (H-bonds are cyan colored), and molecular packing viewed along d) *a*-axis, (e) *b*-axis, and (e) *c*-axis. Zr: yellow, O: red, C: grey, S: orange, N: blue, Cl: green.

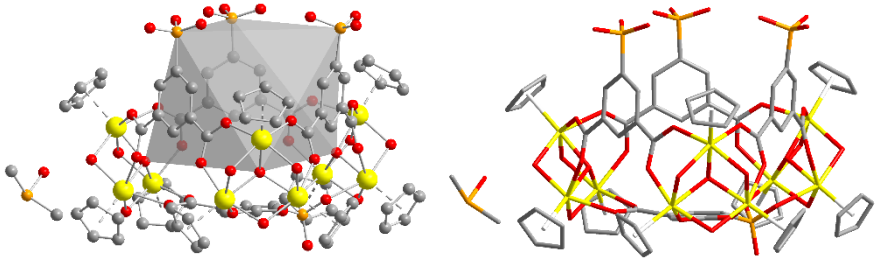

Figure S4. Crystal structure of Na-bound cage recrystallized in DMSO-d_6 and MeOD mixture. DMSO co-crystallized with cage molecules. Zr: yellow, O: red, C: grey, S: orange.

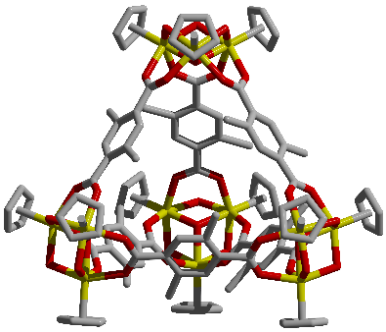

Figure S5. Crystal structure of Zr-dimethyl cage. Zr: yellow, O: red, C: grey. H and Cl atoms are omitted for clarity.

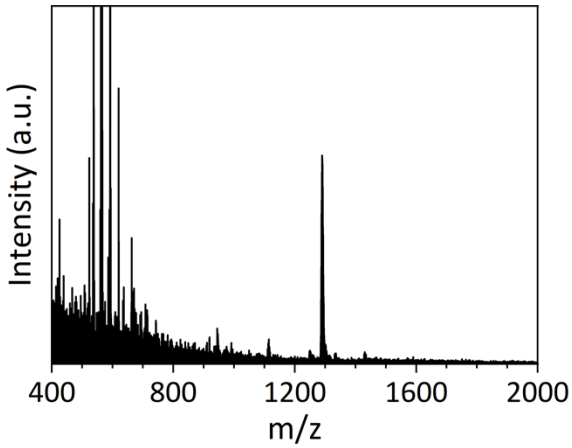

Figure S6. Mass spec spectra of Na-bound cage from 400 to 2000 Da.

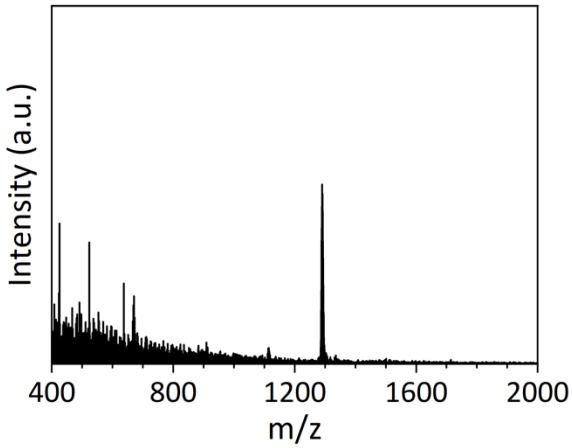

Figure S7. Mass spec spectra of Li-bound cage from 400 to 2000 Da.

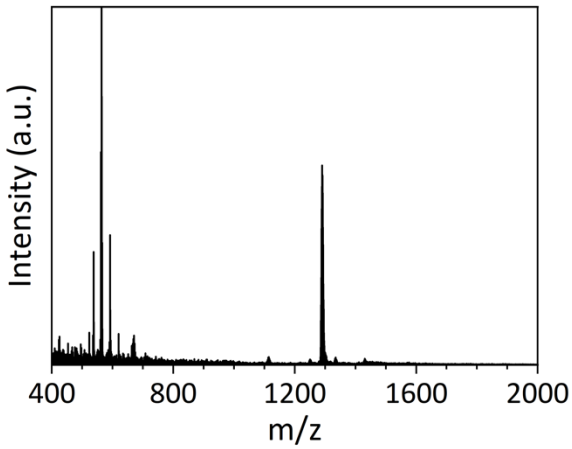

Figure S8. Mass spec spectra of free-pocket cage from 400 to 2000 Da.

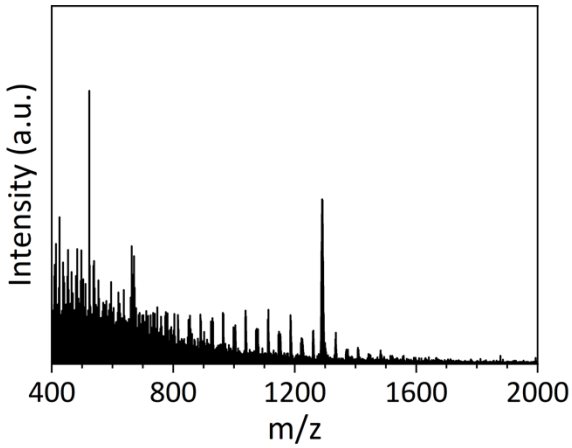

Figure S9. Mass spec spectra of free-pocket cage + NaCl in MeOH from 400 to 2000 Da.

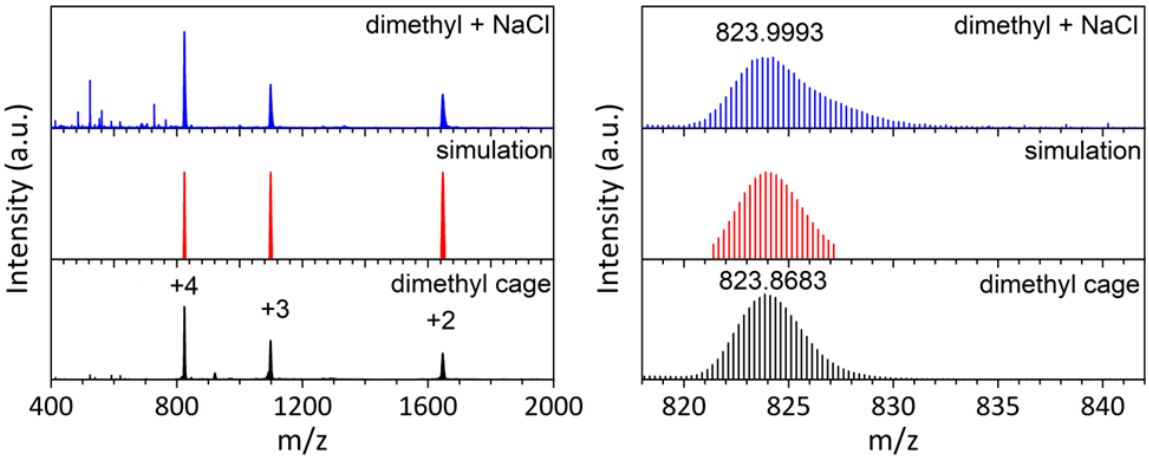

Figure S10. Mass spec spectra of Zr-dimethyl cage and Zr-dimethyl cage + NaCl in MeOH from 400 to 2000 Da (left) and zoomed in +4 peak region (right). The cage +4 peak agreed well with simulation which corresponds to [Zr-dimethyl cage-4Cl^-]$^{4+}$ with a formula of [$Zr_3(\mu_3\text{-}O)(\mu\text{-}OH)_3Cp_3)_4$(2,5-dimethyl-bdc)$_6$].

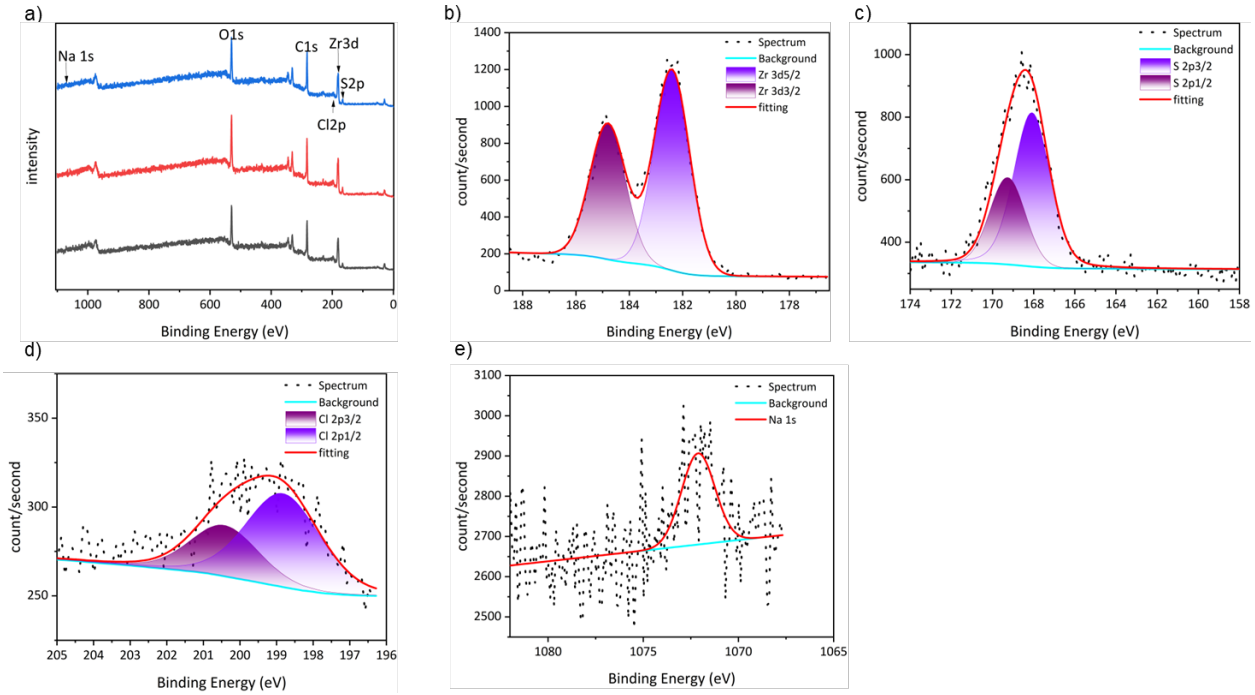

Figure S11. XPS spectra of Na-bound cage. For all XPS spectra, binding energy was calibrated to C1s (284.80 eV).

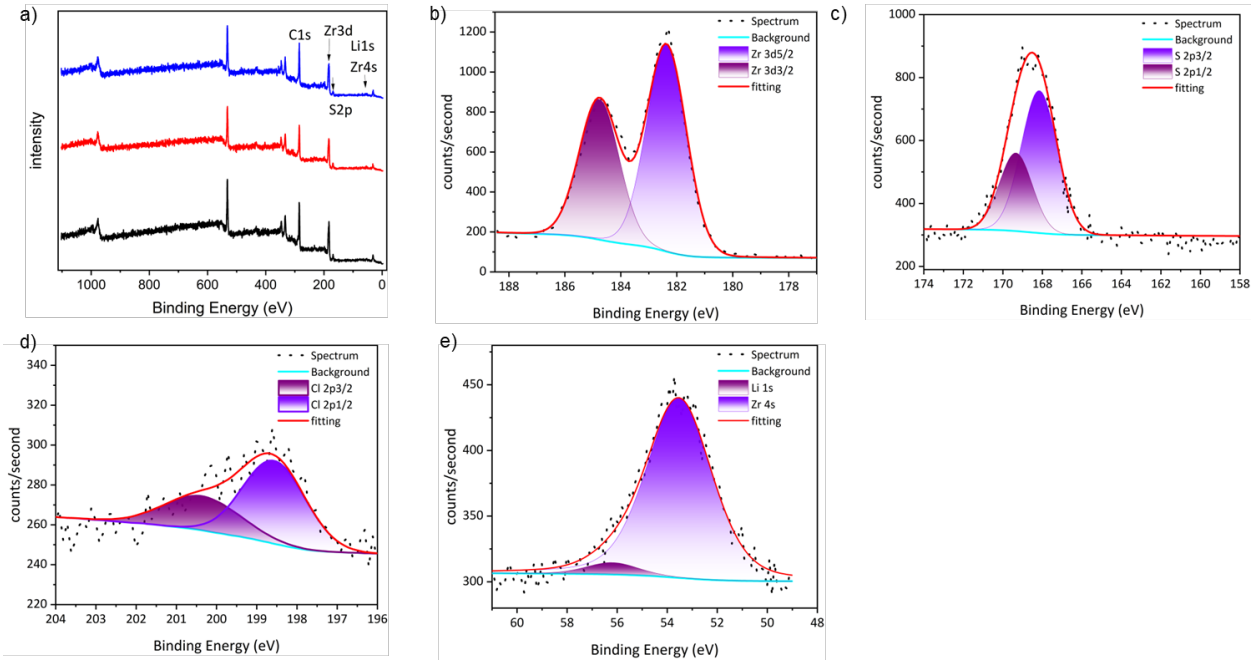

Figure S12. XPS spectra of Li-bound cage.

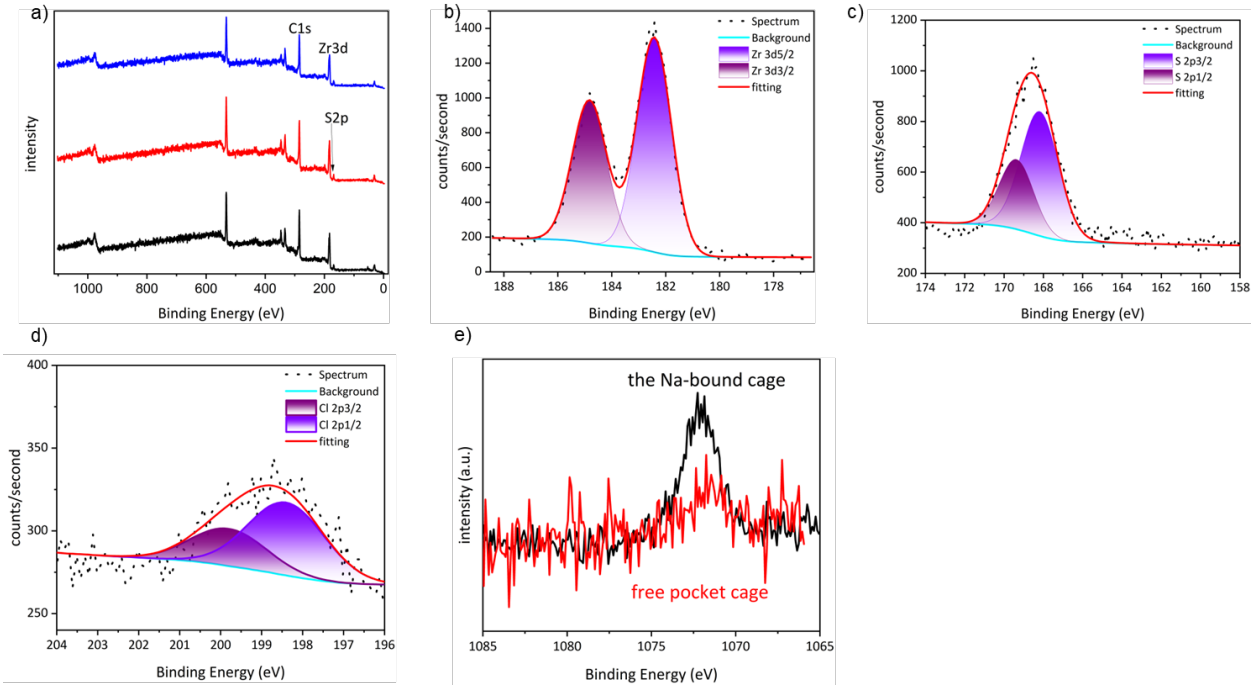

Figure S13. XPS spectra of free-pocket cage. Zr3d spectra was normalized in panel e.

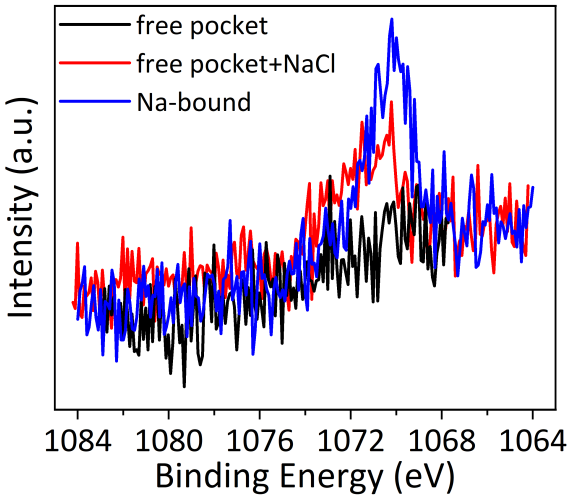

Figure S14. XPS Na1s spectra of free-pocket cage, free-pocket cage+ NaCl and Na-bound cage comparison. Zr3d spectra of these three was normalized.

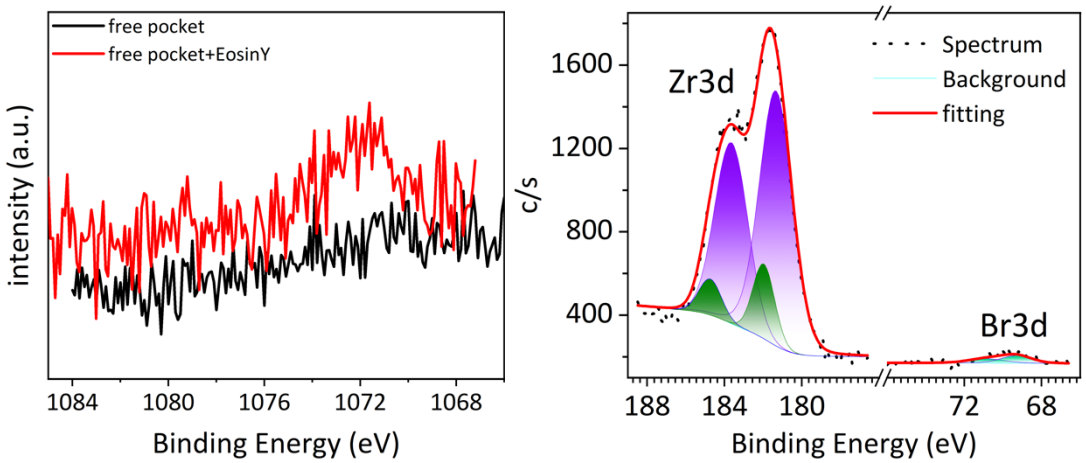

Figure S15. Left: XPS Na1s spectra of free-pocket cage and salt made from free-pocket cage and Eosin Y. Zr3d spectra was normalized. Right: XPS spectra of Zr3d and Br3d for salt made from free-pocket cage and Eosin Y.

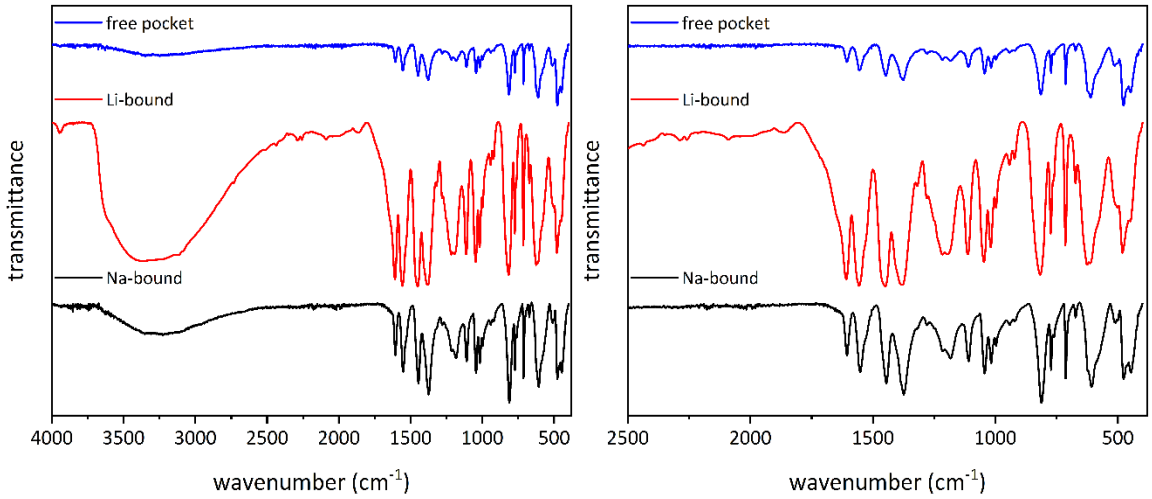

Figure S16. IR spectra of Na-bound, Li-bound and free-pocket cages (left) and zoomed in from 2500-400 cm^{-1} (right).

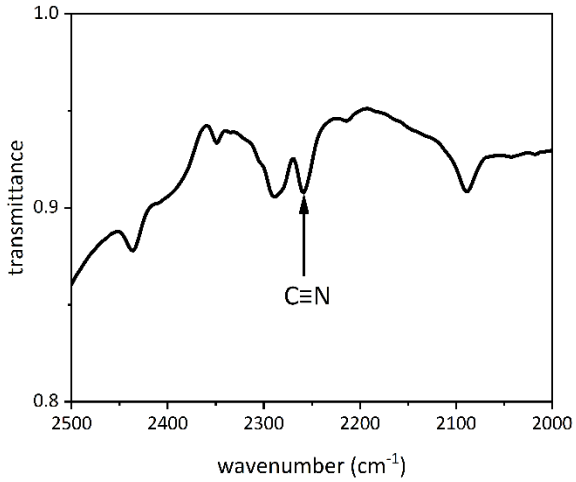

Figure S17. IR spectra of Li-bound zoomed in from 2500-2000 cm^{-1}.

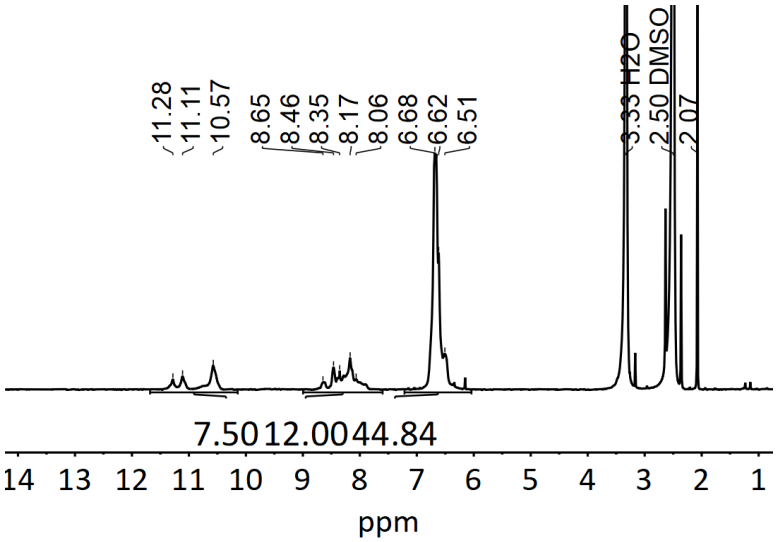

Figure S18. ^{1}H NMR (500 MHz) of Na-bound cage in DMSO-d_6.

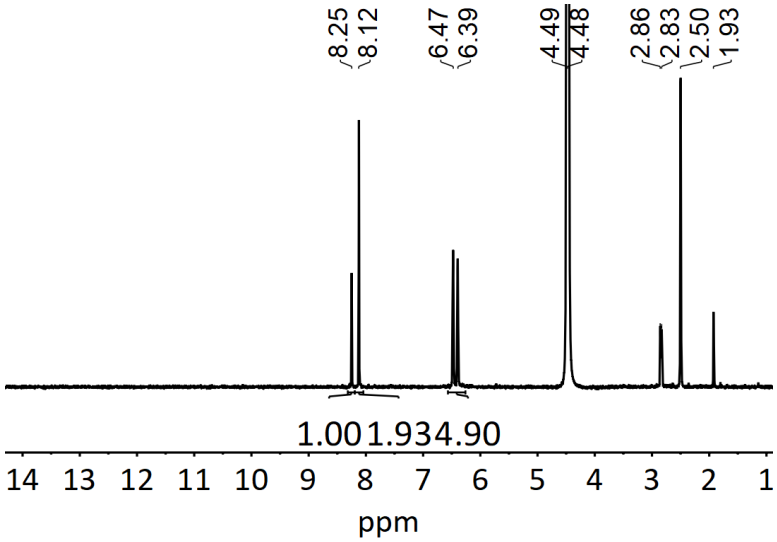

Figure S19. ^{1}H NMR (500 MHz) of Na-bound cage digested with CsF in DMSO-d_6.

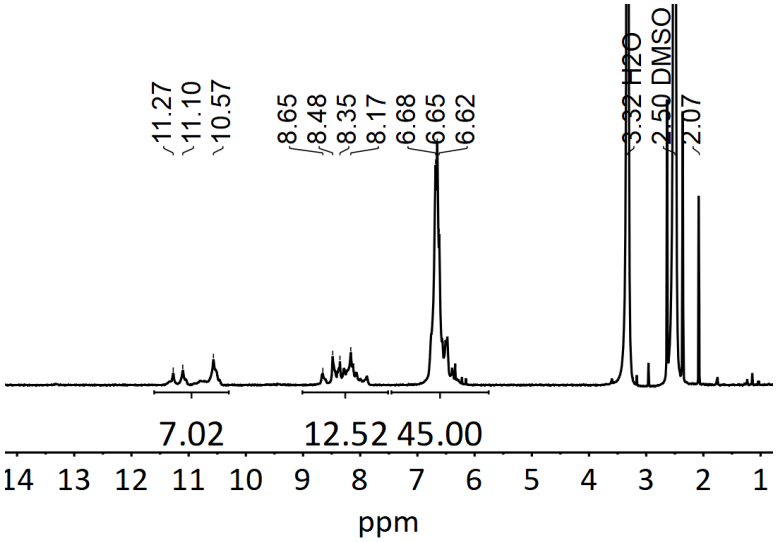

Figure S20. ^{1}H NMR (500 MHz) of Li-bound cage in DMSO-d_6.

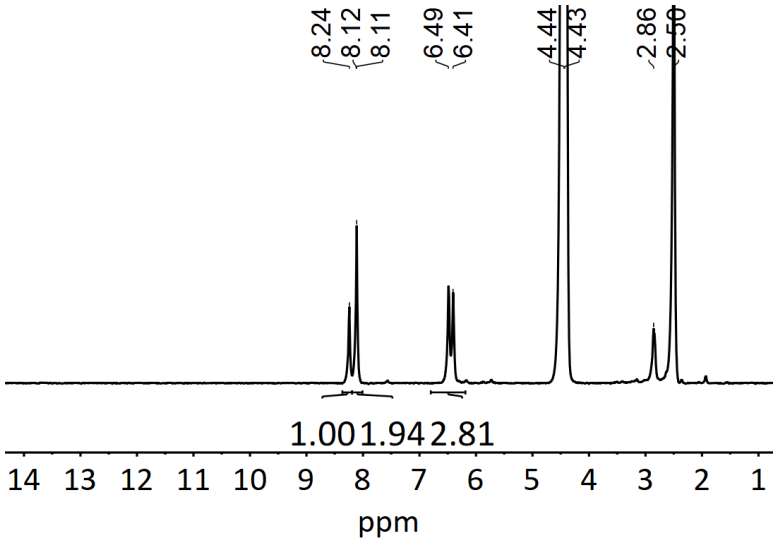

Figure S21. ^{1}H NMR (500 MHz) of Li-bound cage digested with CsF in DMSO-d_6.

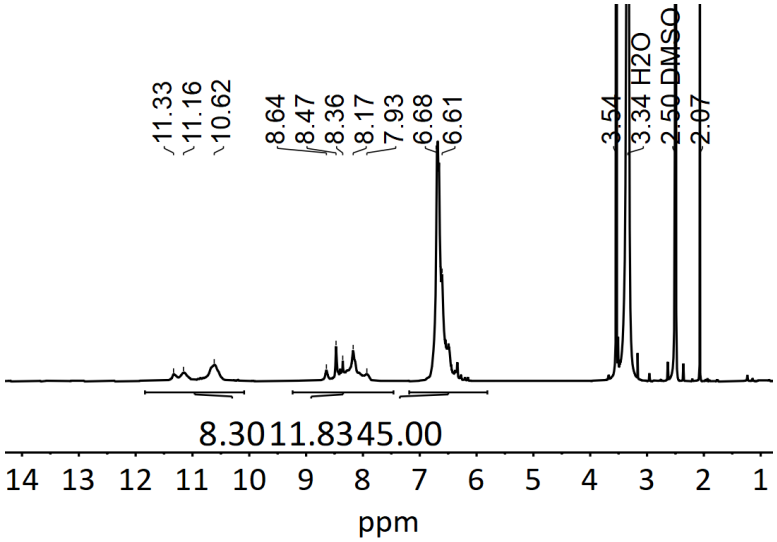

Figure S22. ^{1}H NMR (500 MHz) of free-pocket cage in DMSO-d_6.

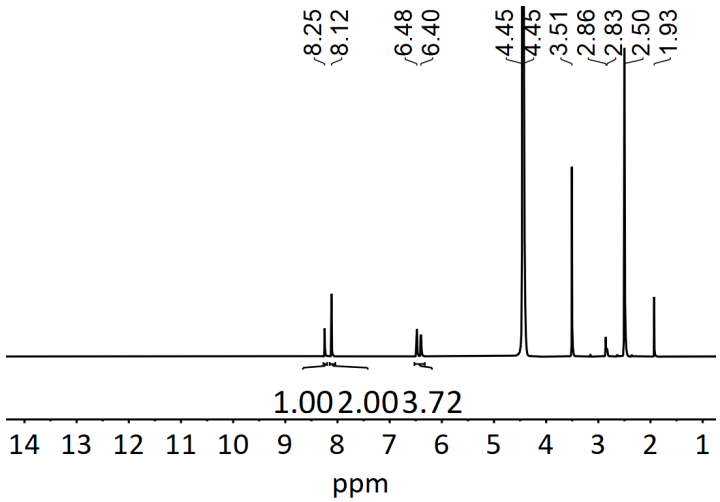

Figure S23. ^{1}H NMR (500 MHz) of free-pocket cage digested with CsF in DMSO-d_6.

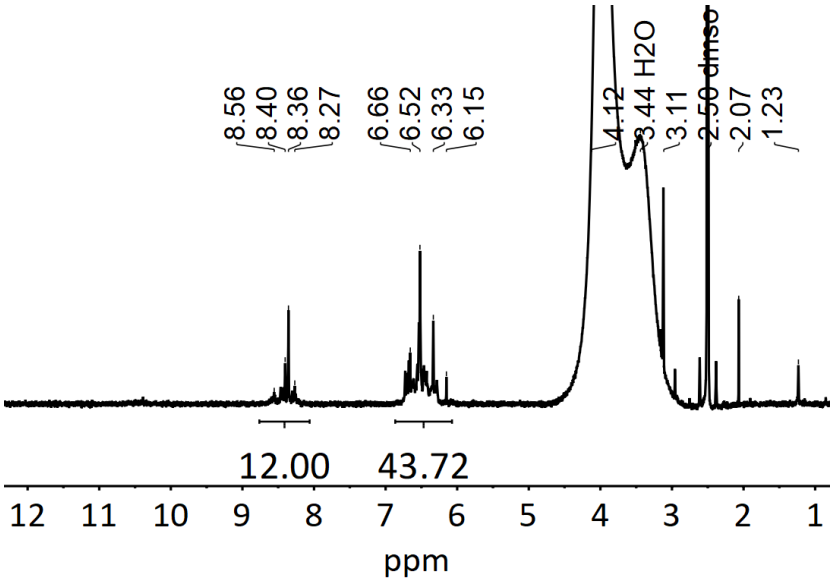

Figure S24. ^{1}H NMR (500 MHz) of Na-bound cage recrystallized in DMSO-d_6 and MeOD mixture and then redissolved in DMSO-d_6.

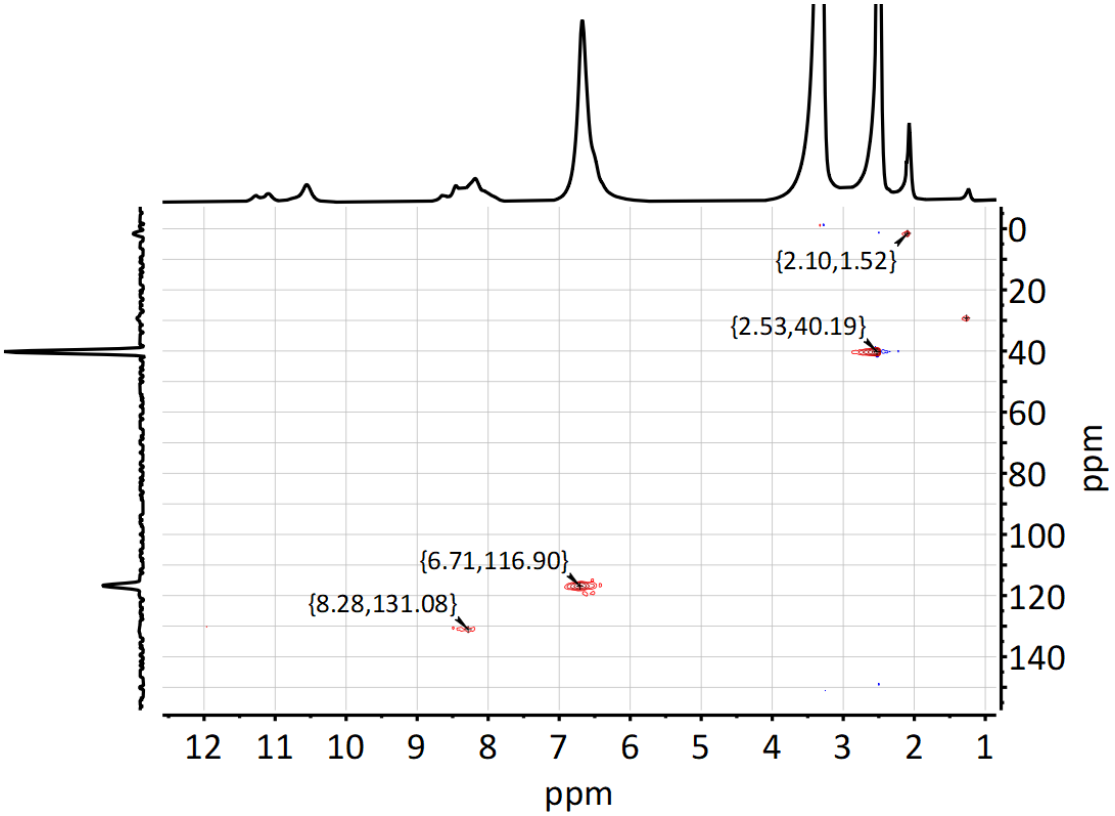

Figure S25. ^{1}H-^{13}C HSQC NMR (500 MHz) of Na-bound cage in DMSO-d_6.

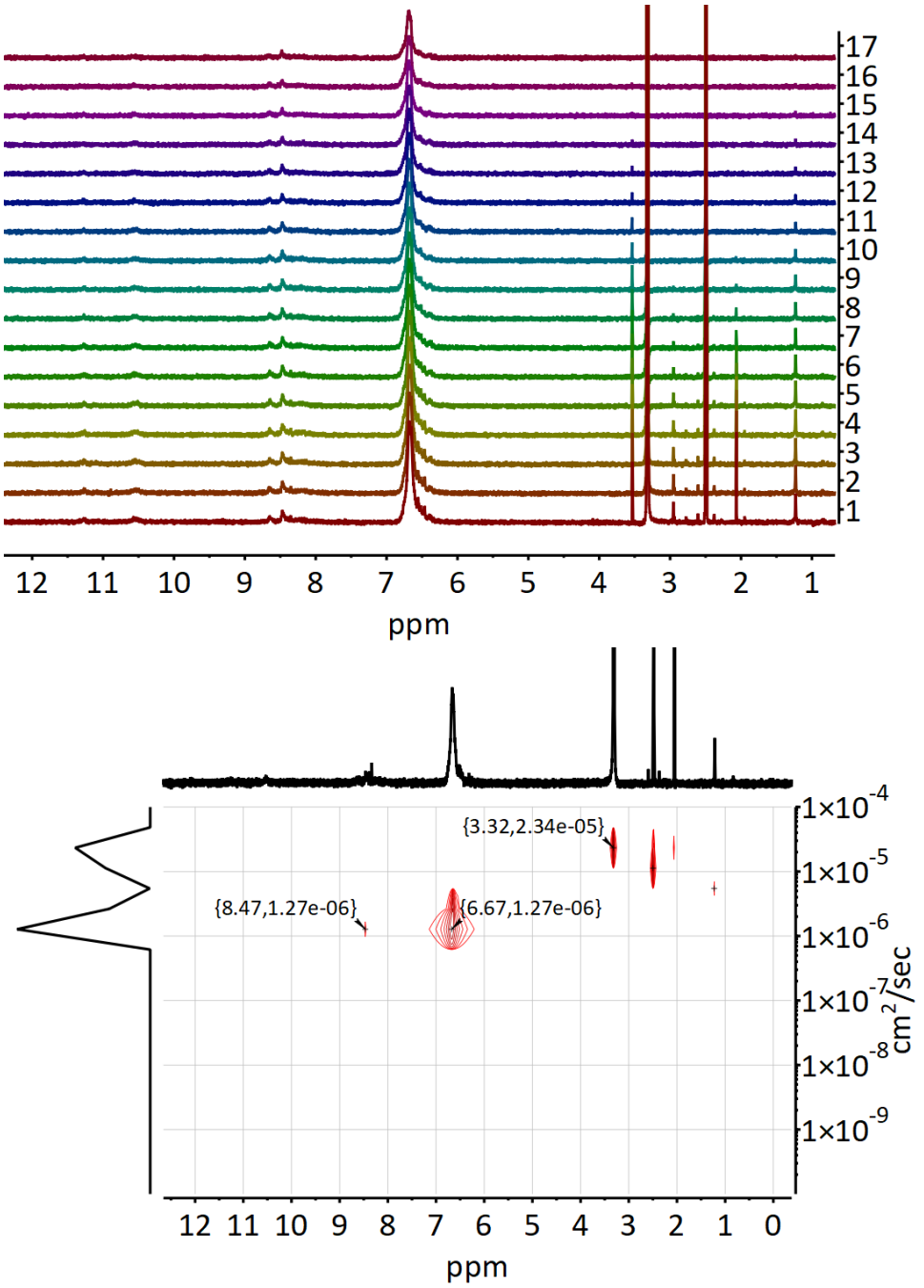

Figure S26. 2D DOSY NMR (500 MHz) of free-pocket cage in DMSO-d_6.

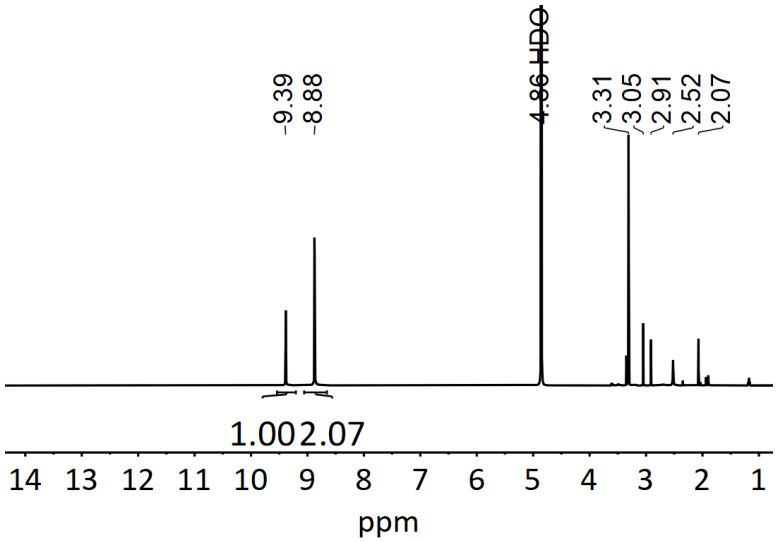

Figure S27. ^{1}H NMR (500 MHz) of $Li_{24}[Mo_{24}(5\text{-}SO_3\text{-}bdc)_{24}]$ cage in MeOH-d_4.

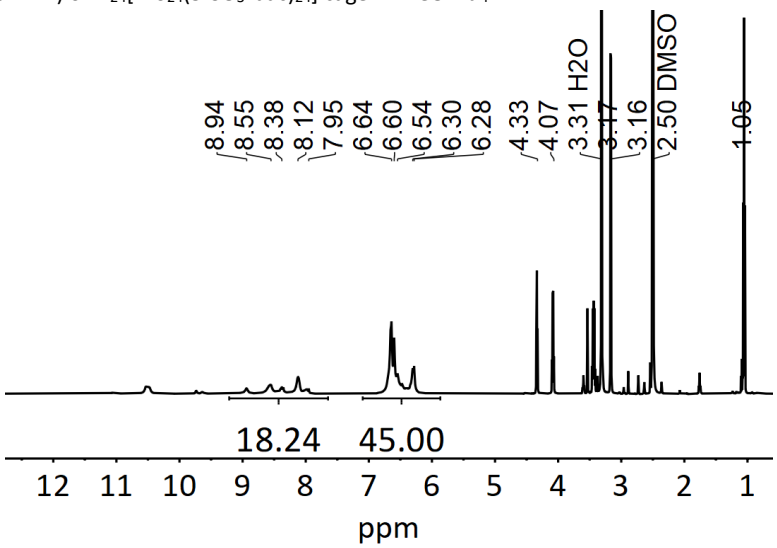

Figure S28. ^{1}H NMR (500 MHz) of the porous salt made from free-pocket and $Li_{24}[Mo_{24}(5\text{-}SO_3\text{-}bdc)_{24}]$ cage in DMSO-d_6.

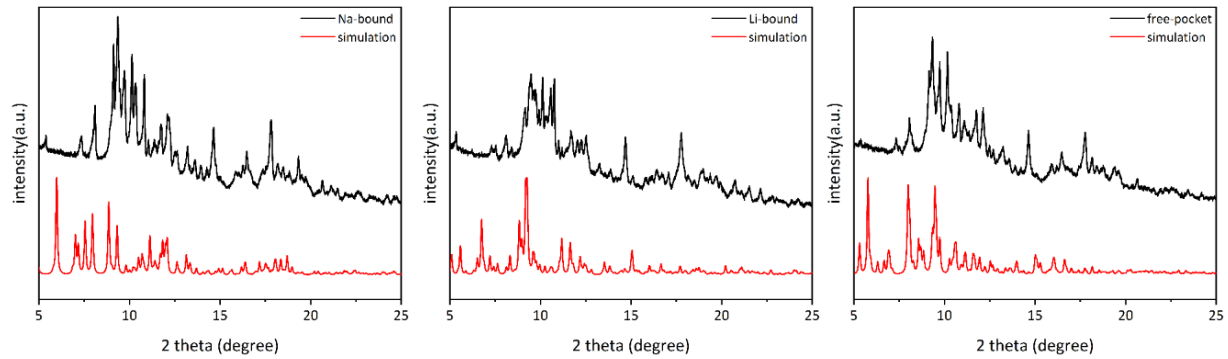

Figure S29. PXRD pattern of Na-bound, Li-bound and free-pocket cage.

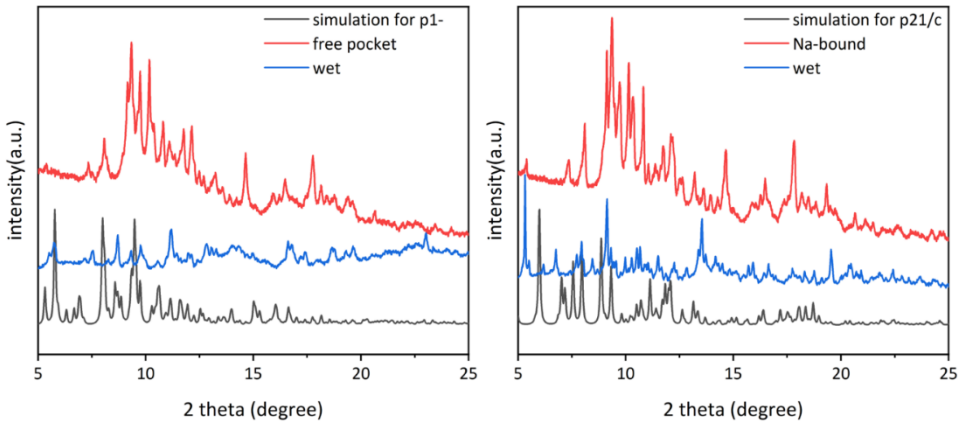

Figure S30. PXRD pattern of free-pocket and Na-bound cage immersed in MeCN mother liquor.

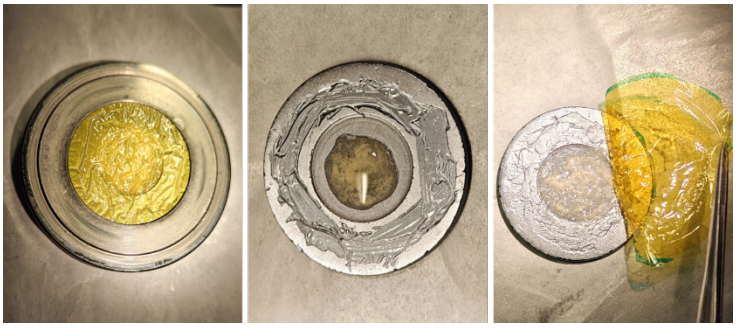

Figure S31. Optical images of cage solids immersed in MeCN mother liquor for wet pXRD experiments.

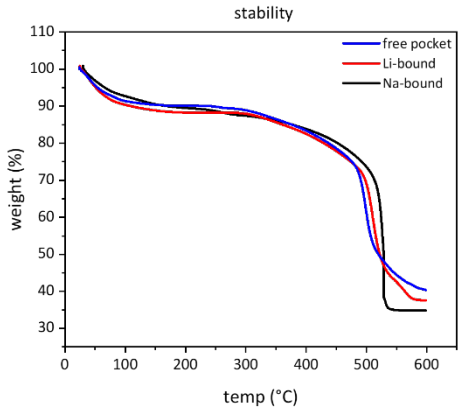

Figure S32. Na-bound, Li-bound, and free-pocket cage heated under simulated air atmosphere (80% N_2, 20% O_2) at a rate of 5 °C/min to 600 °C.

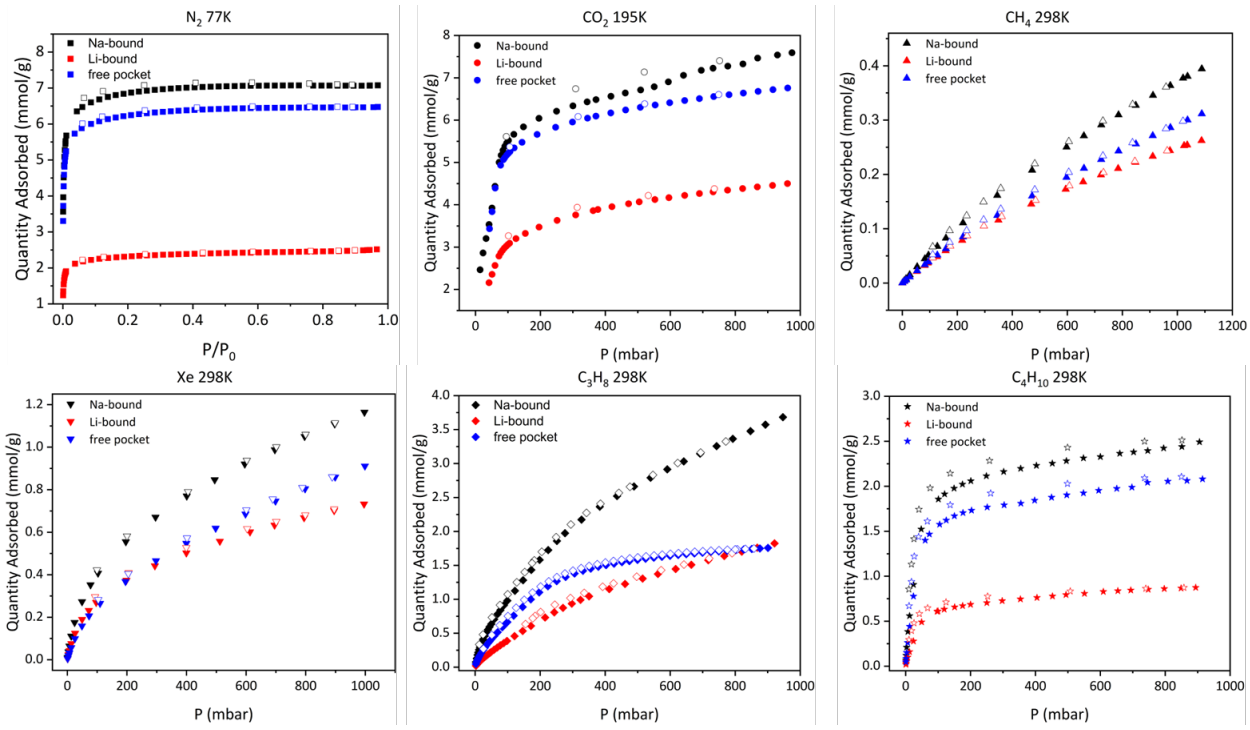

Figure S33. Gas studies of Na-bound, Li-bound and free-pocket cages activated at RT. Kinetic diameter: CO_2 (330 pm) < N_2 (364 pm) < CH_4 (380 pm) < Xe (396 pm) < C_3H_8 (430 pm) < C_4H_{10} (500 pm). Closed and open symbols represent adsorption and desorption, respectively.

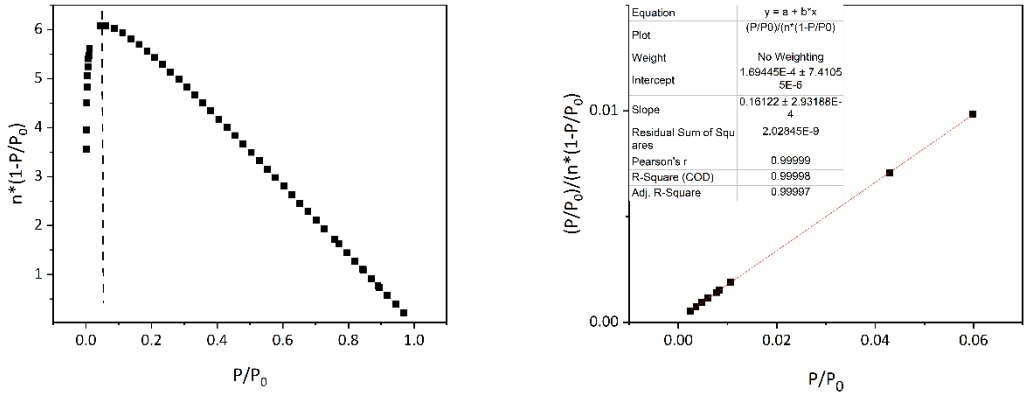

Figure S34. Left: Plot of $n*(1-P/P_0)$ vs. P/P_0 to determine the maximum P/P_0 used in the BET linear fit according to the first BET consistency criterion for N_2 adsorption at 77 K for Na-bound cage activated at RT. Right: The slope of the best fit line for P/P_0 < 0.043 is 0.1612 and the y-intercept Is 0.0002, which satisfies the second BET consistency criterion. This results in a measured BET[Langmuir] surface area of 635[700] m^2/g.

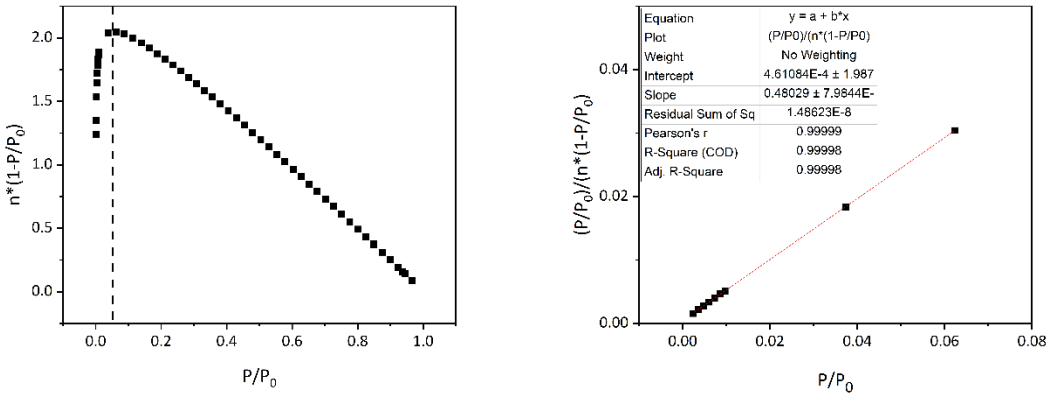

Figure S35. Left: Plot of $n*(1-P/P_0)$ vs. P/P_0 to determine the maximum P/P_0 used in the BET linear fit according to the first BET consistency criterion for N_2 adsorption at 77 K for Li-bound cage activated at RT. Right: The slope of the best fit line for $P/P_0 < 0.062$ is 0.4803 and the y-intercept Is 0.0004, which satisfies the second BET consistency criterion. This results in a measured BET[Langmuir] surface area of 213[241] m^2/g.

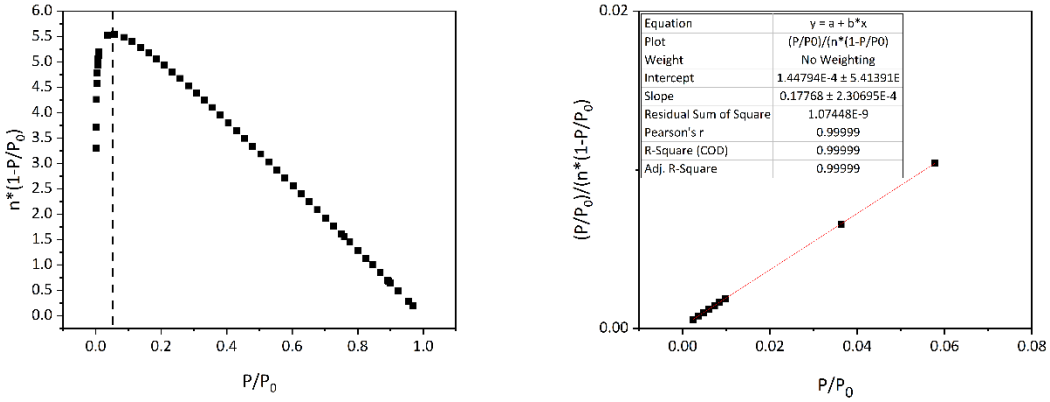

Figure S36. Left: Plot of $n*(1-P/P_0)$ vs. P/P_0 to determine the maximum P/P_0 used in the BET linear fit according to the first BET consistency criterion for N_2 adsorption at 77 K for free-pocket cage activated at RT. Right: The slope of the best fit line for $P/P_0 < 0.058$ is 0.1777 and the y-intercept Is 0.0001, which satisfies the second BET consistency criterion. This results in a measured BET[Langmuir] surface area of 576[639] m^2/g.

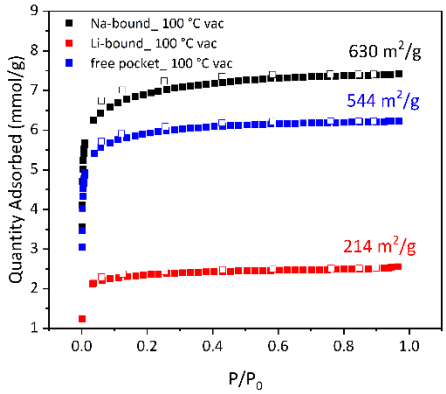

Figure S37. N_2 isotherm at 77 K of Na-bound, Li-bound, and free-pocket cages activated at 100°C. Closed and open symbols represent adsorption and desorption, respectively.

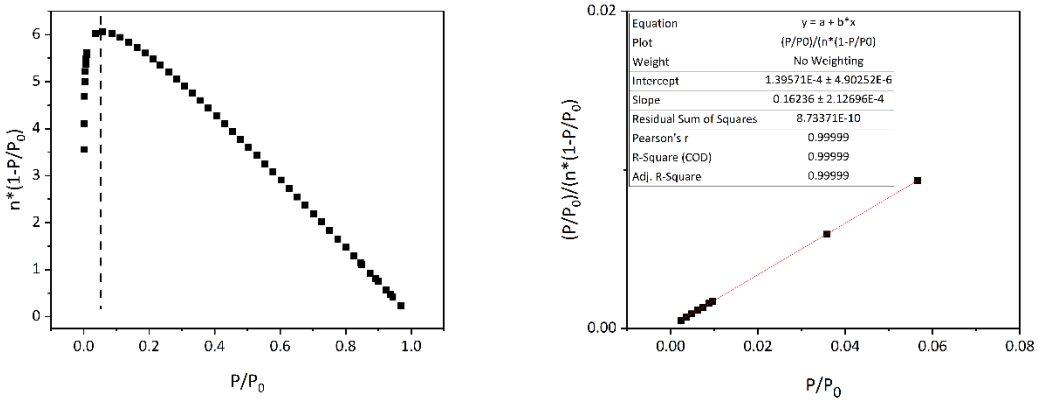

Figure S38. Left: Plot of $n*(1-P/P_0)$ vs. P/P_0 to determine the maximum P/P_0 used in the BET linear fit according to the first BET consistency criterion for N_2 adsorption at 77 K for Na-bound cage activated at 100°C. Right: The slope of the best fit line for $P/P_0 < 0.057$ is 0.1624 and the y-intercept is 0.0001, which satisfies the second BET consistency criterion. This results in a measured BET[Langmuir] surface area of 630[729] m^2/g.

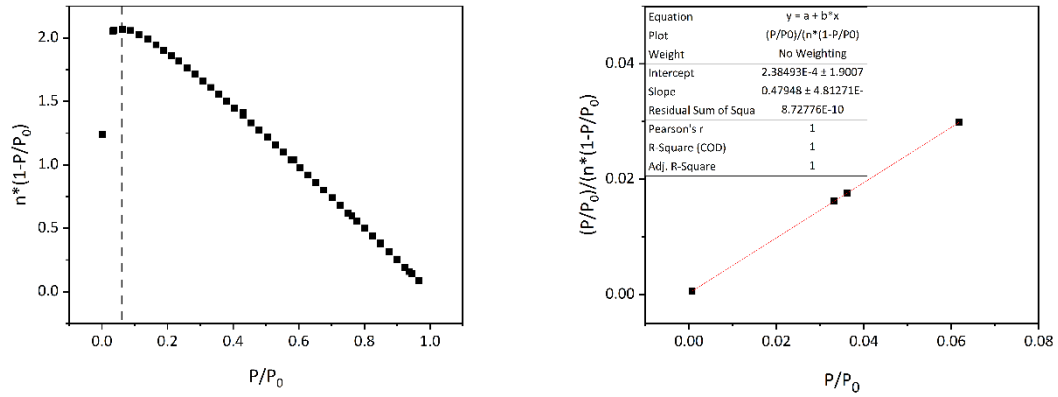

Figure S39. Left: Plot of $n*(1-P/P_0)$ vs. P/P_0 to determine the maximum P/P_0 used in the BET linear fit according to the first BET consistency criterion for N_2 adsorption at 77 K for Li-bound cage activated at 100°C. Right: The slope of the best fit line for $P/P_0 < 0.062$ is 0.4795 and the y-intercept Is 0.0002, which satisfies the second BET consistency criterion. This results in a measured BET[Langmuir] surface area of 214[245] m^2/g.

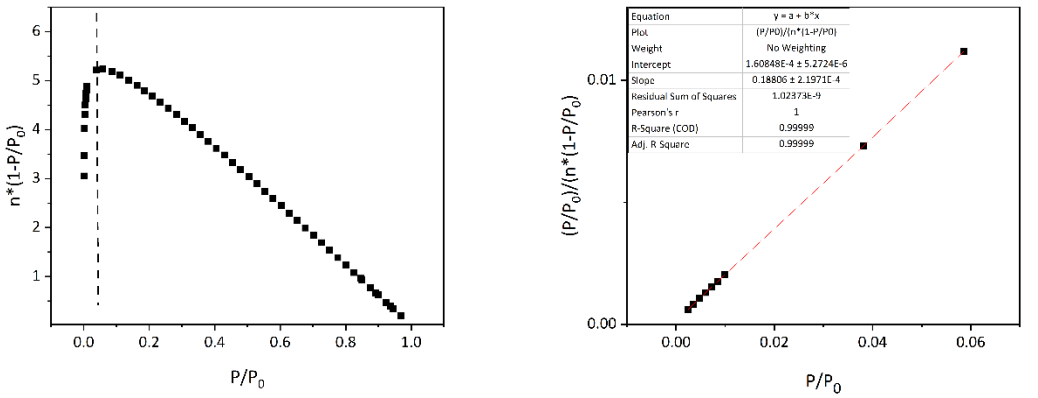

Figure S40. Left: Plot of $n*(1-P/P_0)$ vs. P/P_0 to determine the maximum P/P_0 used in the BET linear fit according to the first BET consistency criterion for N_2 adsorption at 77 K for free-pocket cage activated at 100°C. Right: The slope of the best fit line for $P/P_0 < 0.059$ is 0.1881 and the y-intercept Is 0.0002, which satisfies the second BET consistency criterion. This results in a measured BET[Langmuir] surface area of 544[611] m^2/g.

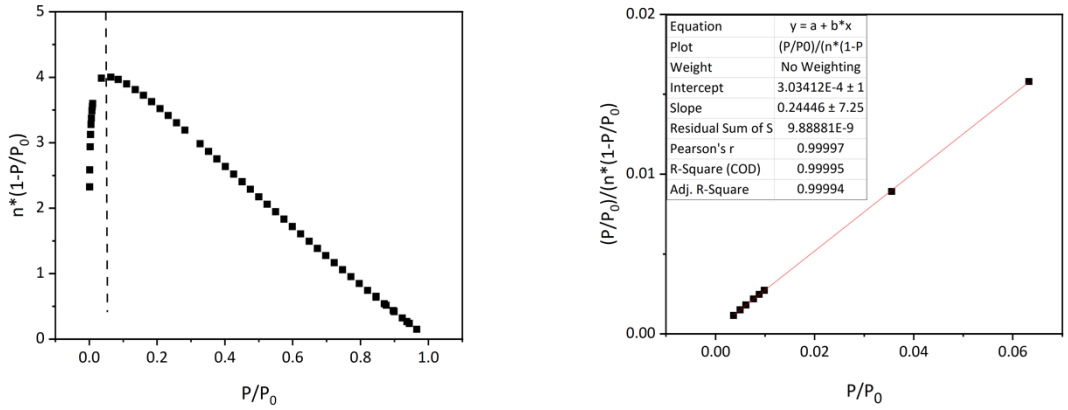

Figure S41. Left: Plot of $n*(1-P/P_0)$ vs. P/P_0 to determine the maximum P/P_0 used in the BET linear fit according to the first BET consistency criterion for N_2 adsorption at 77 K for the porous salt made from free-pocket cage and Eosin Y dye activated at RT. Right: The slope of the best fit line for $P/P_0 < 0.063$ is 0.1881 and the y-intercept Is 0.2445, which satisfies the second BET consistency criterion. This results in a measured BET[Langmuir] surface area of 419[418] m^2/g.

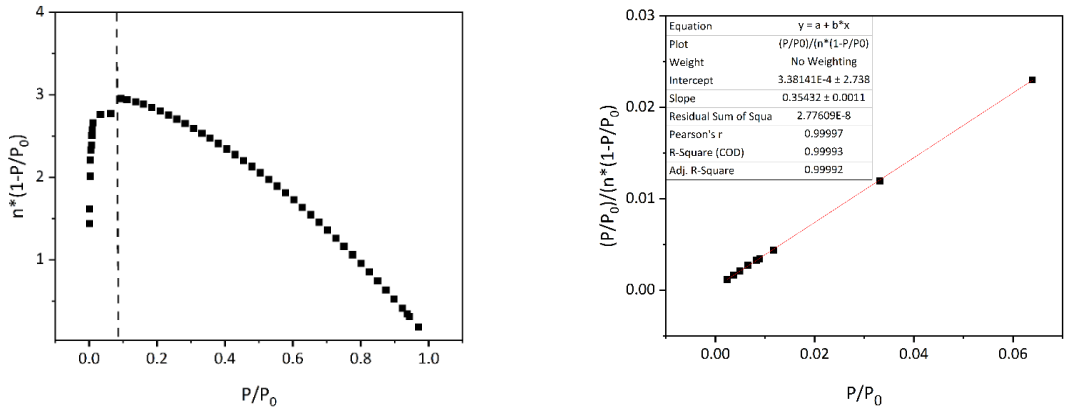

Figure S42. Left: Plot of $n*(1-P/P_0)$ vs. P/P_0 to determine the maximum P/P_0 used in the BET linear fit according to the first BET consistency criterion for N_2 adsorption at 77 K for the porous salt made from free-pocket cage and $Li_{24}[Mo_{24}(5\text{-}SO_3\text{-}bdc)_{24}]$ cage activated at RT. Right: The slope of the best fit line for $P/P_0 < 0.094$ is 0.3543 and the y-intercept Is 0.0003, which satisfies the second BET consistency criterion. This results in a measured BET[Langmuir] surface area of 289[446] m^2/g.

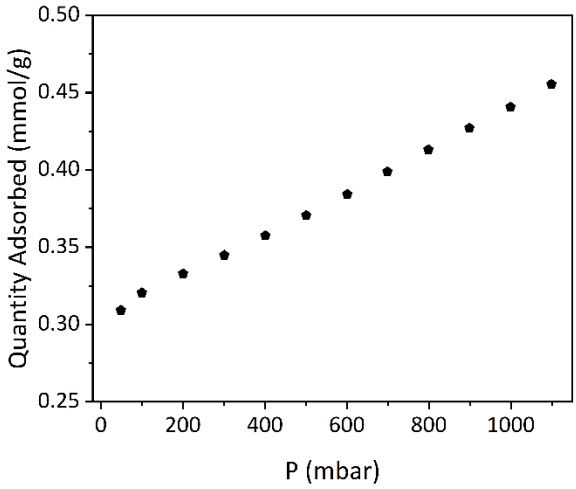

Figure S43. O_2 isotherms at 298 K of the porous salt made from free-pocket cage and $Li_{24}[Mo_{24}(5\text{-}SO_3\text{-}bdc)_{24}]$ cage activated at RT.

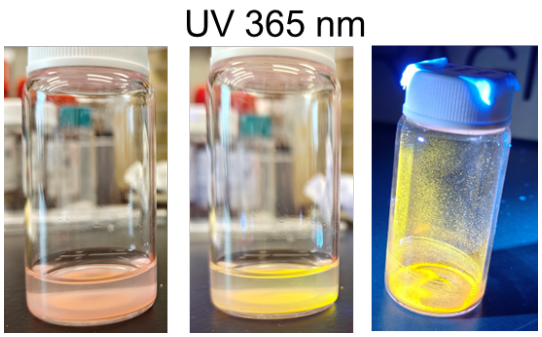

Figure S44. Free-pocket cage reacted with Eosin Y in MeCN for 24 h (left), under 365 nm UV light (middle) and the resulting salt under 365 nm UV light (right).

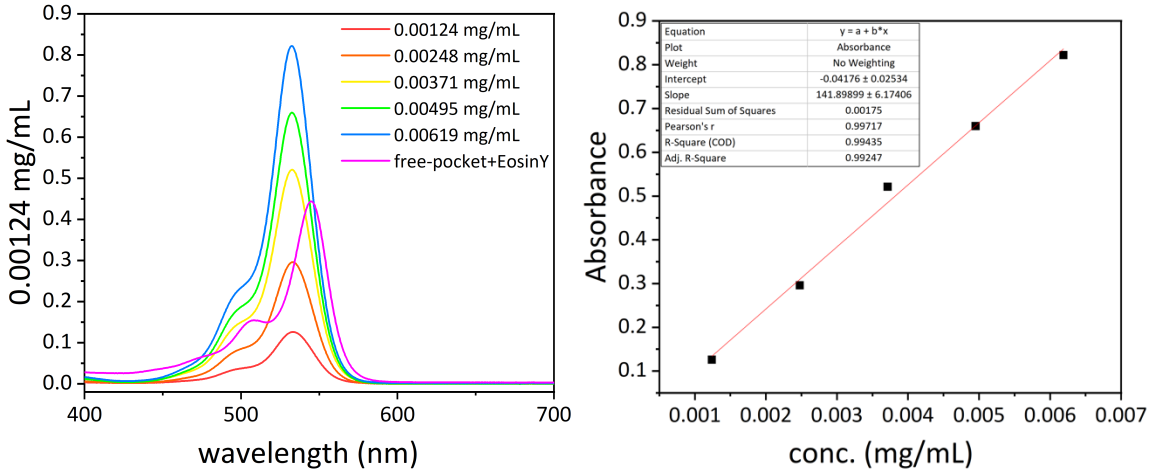

Figure S45. UV-vis of Eosin Y in DMSO (left) and the calibration curve (right). The magenta trace represented the salt sample made from free-pocket and Eosin Y. There was approximately 0.1 dye molecules per cage, equivalent to ~20% occupancy of the tri-sulfonate binding pockets by Na^+.

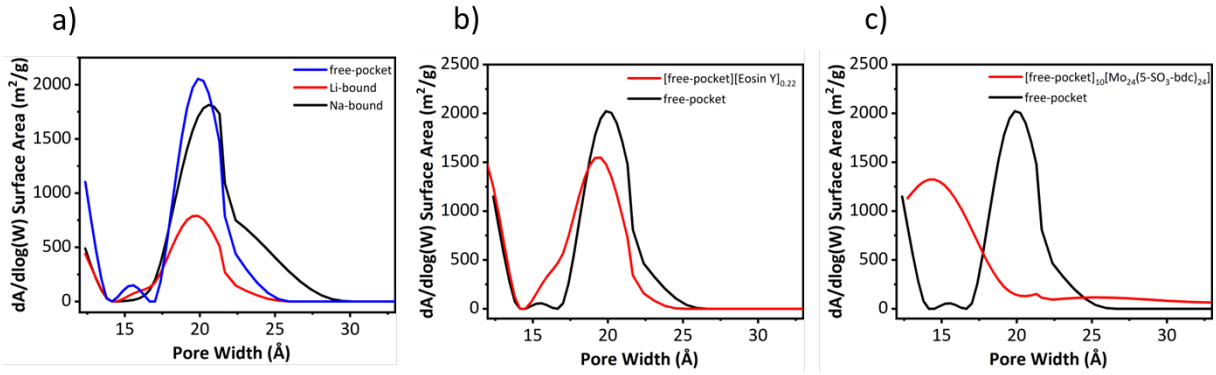

Figure S46. Pore size distributions obtained from NLDFT fitting of N_2 77 K isotherms of a) three cages activated at RT, b) salt made from free-pocket cage and Eosin Y and c) salt made from free-pocket cage and $Li_{24}[Mo(5\text{-}SO_3\text{-}bdc)_{24}]$ cage.

Reference

1. S. Du, G. Liu, M. Zhou, E.M. EI-Sayed, Z. Ju, K. Su and D. Yuan, *Crystal Growth & Design*, 2021, **21**, 692-697.
2. G. R. Lorzing, A. J. Gosselin, B. A. Trump, A. H. P. York, A. Sturluson, C. A. Rowland, G. P. A. Yap, C. M. Brown, C. M. Simon and E. D. Bloch, *Journal of the American Chemical Society*, 2019, **141**, 12128-12138.